Available online at www.sciencedirect.com

ScienceDirect

Transportation Research Procedia 38 (2019) 565–585

Transportation Research Procedia

www.elsevier.com/locate/procedia

23rd International Symposium on Transportation and Traffic Theory, ISTTT 23, 24-26 July 2019, Lausanne, Switzerland

A Behavioral Microeconomic Foundation for Car-following Models

Samer H. Hamdar [a,] * , Vinayak V. Dixit [b], Alireza Talebpour [c] and Martin Treiber [d]

[a] *The George Washington University, 800 22nd Street NW, Washington DC 20052, USA*
[b] *University of New South Wales, Civil Engineering Building (Kensington Campus), Sydney, NSW 2052, Australia*
[c] *Texas A&M University, 301E Dwight Look Engineering Building, College Station TX 77843, USA*
[d] *Technical University of Dresden, Lockwitztalstraße 12, Dresden 01259, Germany*

Abstract

The objective of this paper is to develop a micro-economic modeling approach for car-following behaviors that may capture different risk-taking tendencies when dealing with different traffic conditions. The proposed framework allows for the consideration of perception subjectivity and judgement errors that may lead to unsafe acceleration driving maneuvers with the possibility of real-end collisions. The modeling approach relies on a generalized utility-based formulation with three specific types of subjective utility functions (SUFs): Prospect Utility (PT) subjective utility function, Constant Relative Risk Aversion (CRRA) subjective utility function, and an Exponential Constant Relative Risk Aversion (ECRA) subjective utility function. The formulation is assessed in terms of its homogeneous macroscopic properties (thus leading to a triangular fundamental diagram) and its non-homogeneous microscopic properties (thus leading to realistic following behavior facing different traffic scenarios).

Once tested in terms of feasibility, the modeling approach is calibrated against real-life trajectory data. A Genetic Algorithm (GA) method is adopted to minimize a spacing-mixed-error term while considering inter-driving heterogeneity. The three models (i.e. PT, CRRA and ECRA) produce acceptable error values with the PT model showing the best fit, followed by the ECRA model, followed by the CRRA model. Even though the CRRA and the PT models show similar intensity in the acceleration response to the behavior of a lead vehicle with more disturbance (stochasticity/randomness) seen with the CRRA SUF, the PT and the ECRA models show more realistic wave formation despite their difference in terms of individual acceleration distribution functions. The ECRA model results in an amplified sensitivity to the behavior of the lead vehicle with the acceleration probability distribution function skewed to the left (i.e. towards decelerating rather than accelerating).

The calibration exercise is followed by a simulation exercise. The three suggested models produce a homogeneous congestion phase, but a clear transient single/multiple wave formation is seen with the PT and the ECRA models.

* Corresponding author. Tel.: +1-202-994-6652; fax: +1-202-994-0127.
E-mail address: hamdar@gwu.edu

Peer-review under responsibility of the scientific committee of the 23rd International Symposium on Transportation and Traffic Theory.
10.1016/j.trpro.2019.05.030

These latter models are able to reproduce all the congestion regimes observed on real-world surface transportation networks. The ECRA is characterized by a decreased capacity and increased traffic disturbances with additional shockwave formation. Finally, the different models allow the possibility of perception or judgement errors with the explicit incorporation of a collision probability and a collision weight in the suggested formulation approach.

Peer-review under responsibility of the scientific committee of the 23rd International Symposium on Transportation and Traffic Theory.

Keywords: Calibration; Cognitive; Congestion; Fundamental Diagram; Heterogeneity; Human Factors; Safety

1. Introduction and Motivation

1.1. Motivation

The ultimate goal of this paper is to provide a comprehensive numerically verifiable theory for subjective utility-based car-following models. Car-following is still considered the basic driving maneuver that explains different congestion dynamics and collision formations (NHTSA, 2016; FHWA, 2004). However, in the era of autonomous vehicles, aren't we removing the subjective utility and the human component from the driving process? Why do we need to understand driving behavior in a micro-economic context given that one of the reasons behind the introduction of driver-less cars is the elimination of the human error and thus the reduction of traffic incidents? Interestingly enough, traffic simulation models including microscopic acceleration models have been built naturally to account for vehicle automation rather than human driving decision making processes (Van Lint and Calvert, 2018). Except for the earlier efforts seen in the psychophysical models (Wiedemann and Reiter, 1992 – utilized in the VISSIM traffic simulation tool) and the utility-based models (Ahmed, 1999 – utilized in the MITSIM traffic simulation tool), traffic scientists did not account for terms like emergency behavior, perception indifference, stochasticity and randomness in execution when capturing driving behavior. Most of the driver behavior models including the one-dimensional acceleration models remain deterministic and collision-free (Hamdar, 2015). Some additional efforts have been dedicated to incorporating human decision-making processes into existing traffic models (Treiber et al., 2006). However, very few psychology-based or economics-based constructs have been introduced in order to capture the cognitive dimensions behind some observed maneuvers. These dimensions include fatigue, mental load, risk, sensitivity, stress, and uncertainty. Recently, Human Factor (HF) researchers and traffic flow researchers have been focusing on such terms while trying to account for them in new or existing driving behavior modeling frameworks (Hoogendoorn et al., 2014; Saifuzzaman and Zheng, 2014; Saifuzzaman et al., 2017). This research falls under this category of work where the authors would like to establish a family of car-following models accounting for sensitivity, stochasticity and randomness, risk and uncertainty. These models should be calibrated and validated while reproducing different congestion dynamics and incident-prone behaviours.

Another major motivation behind studying the human decision-making process and the cognitive dimension of driving behavior is associated with the gradual rather than the complete deployment of connected and automated vehicles (CAVs). The CAV technology development aspect is being led by the private sector and different public agencies and governments have been working on devising regulations and tools to secure a positive aggregate CAV impact on traffic mobility and safety. As an example, autonomous vehicles may allow added roadway capacity but may lead to additional vehicle miles traveled (Childress et al, 2015). There is still a lack of data that quantifies the responsiveness and the acceptance of drivers and travelers to connected and automated vehicles. Several predictions have been suggested on the rate of deployment of such vehicles on our roadways. For example, a 2016 report mentions that half of all vehicles will be 'fully autonomous' within the next 10 years (Atkins, 2016). In the same report, 6 levels of automation have been suggested to the United Kingdom (UK) Department of Transport. Level 1 is a zero-automation level where the driving task is fully carried by human drivers. Level 2 involves some basic driving assistance by either steering or accelerating the vehicle based on the surrounding environment. Level 3 indicates partial automation with both steering and acceleration conducted by the auto-pilot system. Level 4 is a conditional automation level where the auto-pilot system may perform all the driving tasks with the possibility of intervention by the human driver. Level 5 is the high automation level where the auto-pilot system is functional even if a human driver does not respond to a request to intervene. Level 6 is a full automation level where the auto-pilot system can perform all aspects of the dynamic driving tasks under all conditions. It is then clear that automation will be introduced gradually in the following decade or two and the human component will play a major role dictating the efficiency of the auto-pilot system especially when a mix of human-driven non-equipped vehicles and full/high/partial/conditional autonomous vehicles are seen in the traffic mix.

1.2. Behavioral Framework and Objectives

Given the need to understand the interaction between the human operator and the vehicles being operated on our roadways, the importance of the cognitive dimensions associated with human decision-making processes should be recognized. Multiple research efforts have been made to understand decision making in multiple contexts including finance, politics, psychology …etc. (Frydman and Camerer, 2016; Mintz and Sofrin, 2017; Barthélemy and Coppin, 2006). With such efforts, decision-making theorists have presented a rich literature of studies tackling topics ranging from utility maximization theory (Hwang and Masud, 1979; Chankong and Haimes, 2008) to game theory (Camerer, 2011). We suggest in this paper that the driver behavior is framed using the human information-processing system introduced by Hastie and Dawes (2010) with a subjective utility component in the working memory perception module and the decision-making judgement module. Adapting such system to the driver behavioral task, Figure 1 may be offered: the *working memory module* and the *decision-making module* are fundamental to the problem addressed in this study.

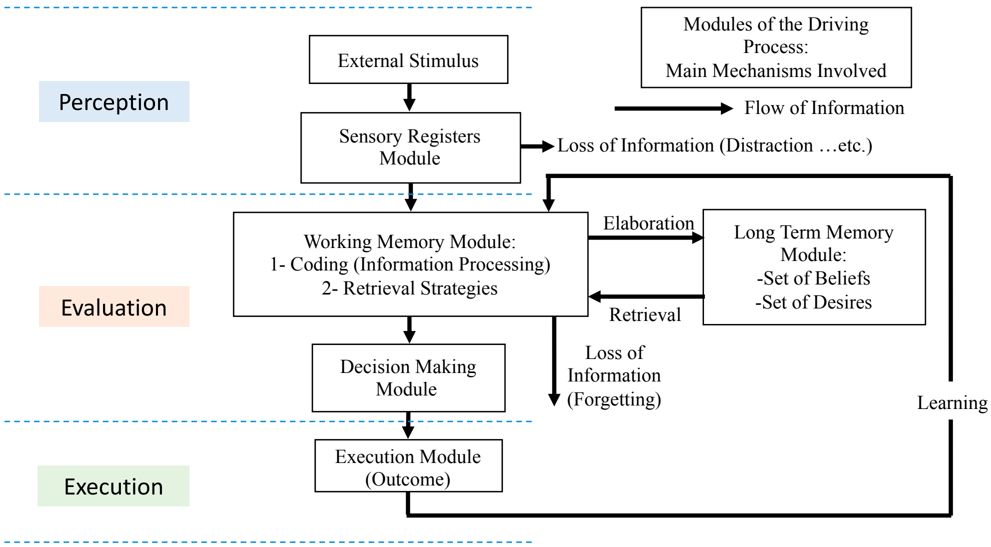

Fig. 1. Information-Processing/Execution System for the Driving Activity.

On the hand, this paper focuses on the operational traveler decision making level (i.e. acceleration and car-following) without accounting for the tactical lane-changing/merging task or the more strategic route choice task, the destination choice task, and/or the departure time choice task (Hranac et al., 2004; Colyar and Halkias, 2007). The driving car-following task involves human decision-making and behavioral processes where *a)* perception, *b)* evaluation and *c)* execution need to be explicitly considered (Figure 1). The evaluation phase involves *1)* uncertainty, *2)* risk-taking, *3)* human errors and *4)* subjectivity leading to a heterogeneous stochastic traffic environment that should be further investigated.

Focusing on the explicit modeling of the evaluation phase and thus a human-centric traffic modeling approach, there seems to be a need to develop rich behavioural models based on micro economic theory (as articulated in Dixit, 2013) and to offer a tool through which we can evaluate policies (insurance, safety, information provision etc.) that can influence driver behavior. In particular, explicit representation of drivers' risk attitudes and perceptions is expected to provide greater insight into the role of risk-taking behaviors in congested and/or accident-prone situations. Earlier work (Hamdar et al., 2008; Hamdar et al., 2009; Hamdar et al., 2015) utilized a prospect theory approach to develop, calibrate and evaluate a behavioural car-following model. However, there are different families of utility functions that capture different characteristics of risk attitudes and have different numerical properties that could have significantly different implications on traffic flow dynamics. Accordingly, a more comprehensive modeling effort is needed where the objectives are:

(i) to develop a general utility-based framework for car-following;

(ii) to evaluate the macroscopic and microscopic traffic properties of car-following models developed using different utility functions;

(iii) and to develop a calibration method to estimate the parameters of these models while capturing different heterogeneity patterns.

Given the aforementioned motivations, framework and objectives, this paper is organized as follows. Section 2 offers a brief literature on decision making theories, their characteristics and their applicability to driver behavioral modeling. Section 3 presents the micro-economic formulation of the car-following task and the associated macroscopic and microscopic feasibility. The data adopted and the calibration method are shown in Section 4. Section 5 offers the numerical results and analysis before concluding with a summary of the findings and some suggested future research directions in Section 6.

2. Literature Review

A significant amount of transportation research has been conducted to understand and to model traveler decision-making processes (Bhat and Steed, 2002; Jaber and O'Mahony, 2009; Mahmassani and Liu, 1999; Mahmassani et al., 2013; Walting and Cantarella, 2015). However, limited work has been successful in applying decision making theories at the driver behavioral operational level (Hamdar et al., 2015). Accordingly, in this section, we review existing decision-making theories that may be adapted by transportation researchers to capture decision making under uncertainty/risk. Such modeling approaches are classified into three types: a) Expected Utility Theories and Their Refinements, such as Prospect Theory, b) Process Theories of Cognitive Decision Making, and c) Multi-Stakeholder Theories, such as Game Theory.

<u>Expected Utility Theories and Their Refinements:</u> these approaches are based on the premise that travelers/drivers can never be certain about the future outcomes of their choices. Given this assumption, multiple theories for modeling choices under uncertainty have been suggested. Out of these, three main theories (as defined by transportation researchers) may be applicable to transportation decision-making, namely: *i)* Expected Utility Theory (EUT), *ii)* Prospect Theory (PT) and *iii)* Regret Theory (RT) (Moraes Ramos et al., 2014). The core assumption of EUT is that decision makers have context-independent preferences and use them to assess all probable outcomes when confronted with a decision set; for EUT to work, these preferences must be stable over time and lead people to choices that maximize their own utility (i.e., best outcome value, best payout, etc.). However, there is a large body of literature suggesting people do not make decisions in this manner motivating additional refinements on the EUT formulation leading to PT (Moraes Ramos et al., 2013, Xue et al., 2011). PT is a refinement of EUT that aims to describe real-world decision-making by assuming that choices reflect gains or losses relative to a reference point. This has been used to describe decisions in a manner that is more psychologically accurate than other formulations, such as EUT, which assume that choices are optimal. The original formulation of PT suggests that decision-making processes occur in two stages: a) the Editing Stage, where decision rules are used to frame possible outcomes in gains or losses relative to a neutral reference point and b) the Evaluation Stage where the decision-maker evaluates the edited potential outcomes of all alternatives according to a value function that incorporates subjective probabilities. RT is based on the idea that a choice from a set of alternatives is not only based on the anticipated payoff of the chosen alternative, but also the anticipated payoff of the alternatives that have not been chosen. Regret is motivated by the possibility that one of the non-chosen alternatives could have had a greater payoff compared to the chosen alternative; in other words, it is the mental block of "what could occur given a different choice is made" that can motivate decision-making (Rasouli and Timmermans, 2014). Rejoice, the opposite of regret, occurs when the chosen alternative results in the

greatest payoff. People make decisions in an effort to maximize rejoice and minimize regret. A differentiating factor for RT is that the decision reference point includes the entire choice set, and there is no context dependency per se, as with PT. In this paper, the focus is on EUT and PT based modeling. RT has its relevance and has also been argued for in different disciplines (Gerbert, 2002; Strack and Viefers, 2014). Multiple researchers have also adopted RT in transportation related applications (Chorus, 2012; Moraes Ramos et al., 2011; Ramos et al., 2018). However, these adoptions have focused on strategic traveler decision making processes (i.e. route choices). Moraes at al. (2014) did find that both PT and RT are suitable for traveler decision making modeling. Accordingly, this paper does not argue that RT is more (or less) valid than PT either in terms of capturing human decision making or in terms of the translatability of the theory into an efficient traffic simulation tool/model. The objective of this paper is to offer a utility-based construct to build acceleration behavior models that may be calibrated, validated and efficiently simulated while capturing the uncertainties associated with the driving tasks, particularly car-following tasks. In fact, within such a construct, RT can be framed for acceleration choice modeling.

All of these "theories" assume that decisions are represented in a rational manner, a key assumption in this paper. It should be noted however that decision-makers may encode multiple different levels of mental representation into the decision-making process, differentiating between what is "seen" and what is "perceived". This allows for the incorporation of meaning, such that decisions can vary with surrounding environmental and socio-demographic factors.

Process Theories of Cognitive Decision Making: Process theory classifies "thinking" into two categories: *i)* a fast and intuitive thinking; and *ii)* a slow and deliberate thinking. Accordingly, two forms of processing contribute to the behavior of a given decision-maker and thus the existence of a dual processing system. Stanovich et al. (2014) offer a general review of dual processing dichotomies with a clear distinguishing between the characteristics of the two aforementioned types of thinking and thus the processing. The first type of processing (named Type 1) is automatically triggered when stimuli are encountered (e.g., "bottom-up, intuitive, automatic responses"), and its automatic nature defines its features: Type 1 processing is very basic in the amount of cognitive demand it requires (e.g., "automatic responses are easy"). On the other hand, the second type of processing (named Type 2) has its feature associated with the ability to accommodate a "decoupling of mental representations from other processing". Such representations carry out "mental simulations" or complement other types of higher level non-automatic actions to aid in the making of the "suitable" decision(s). The decoupling utilizes the working memory and is associated with a longer decision-time: the decoupling implies a higher-level processing taking the mental representation offline for more processing of the representations that are triggered by automatic processing. This dual process model is expanded further to account for individual differences leading to the tripartite model (Stanovich, 2012; Stanovich et al., 2014). The tripartite model accounts for individual differences in a way that illustrates effects in judgments in decision making across three interconnected modules. These modules are:

(i) Thinking disposition (e.g., "beliefs about efficiencies of alternative choices, reflective, internally regulated, goal prioritization, epistemic beliefs, willingness to change one's mind, open-mindedness, consciousness, diligence"). It should be noted that the measures of intelligence have limited established relationship with some thinking dispositions (Stanovich, 2012).

(ii) Fluid Intelligence (e.g., "technical problem solving, doing math, etc.").

(iii) Autonomous responses (e.g., "pre-attentive processing, salience, actions learned to automaticity"). It should be noted that individual differences (i.e. inter-decision-makers' heterogeneity) are reported to be less significant in this module and very prominent in the two above. It should be also noted that this family of theories (i.e. *Process Theories of Cognitive Decision Making*) is the type of theory illustrated in Figure 1.

Game Theory: Game Theory was designed to capture the essence of *strategic* decision-making, and therefore underlies a significant body of agent-based modeling work. The possible collaboration between agents and the flexible modeling framework may have contributed to the recent adoption of the game-theory approaches for modeling traveler behavior (Iyers et al., 2014; Jiang et al., 2014) especially when dealing with the critiqued equilibrium assumption (Easley and Kleinberg, 2010). Even though designed mainly for the strategic decision-making level, additional work have adopted a game theoretic approach to analyze the operational crossing behavior (Arbis et al., 2016) and the tactical lane-changing (Talebpour et al., 2015) behavior. Game theory may also be used to model real-world interactions as re-created in a gaming environment. For example, Roth (2002) notes that game theory can be used to model complex real-world decision-making situations. The major critique of Game Theory has been the extent to which it is externally valid and transferable. Indeed, whenever researchers generate results from a laboratory or a controlled behavioral experiment, external validation is needed to generalize the results to real-life non-controlled environments (Guala & Mittone, 2005). Furthermore, most game-theoretic agents rely on EUT-based decision rules. Therefore, the critiques of EUT apply equally to game theory.

How can the aforementioned decision-making concepts/theories be useful in this paper? A hybrid formulation approach is adopted. For most drivers, *Theories of Choices under Uncertainty* (i.e. Expected Utility Theory, Regret Theory and Prospect Theory) seem to offer a micro-economic comprehensive construct to measures losses and gains in a given driving environment. Accordingly, at the evaluation phase, the Expected Utility Theory and the Prospect Theory (which are seen as the foundation of the micro-economic utilitarian field) are proposed. The Regret Theory may be adopted at a later stage but is still seen as a variant of the Expected Utility Theory with the construct offered in the following formulation section. The micro-economic modelling approach is suitable to describe how a driver perceives, evaluates information, and makes decision for the acceleration rate. The approach is developed based on extensive knowledge in the area of people decision making and there is value in this type of behavioural modelling approach as the current literature in car-following models largely lacks driver behaviour elements.

On the other hand, as implied by 1, *The Processes Theory of Cognitive Decision Making* possibly accounts for a larger number of cognitive dimensions but lacks the foundational tractable structure to translate the underlying variables into an efficient implementable car-following model. In this paper, we suggest focusing on the evaluation phase of the decision-making process, but further extension of this work may be offered to account for additional modules using *The Processes Theory of Cognitive Decision Making* framework. Such extension is beyond the scope of the paper.

3. Methodology

3.1. Formulation and Macroscopic Derivation

The modelling framework utilizes an expected utility maximization framework. Similar to earlier work (Hamdar et al., 2008; Hamdar et al., 2009; Dixit, 2013; Hamdar et al., 2015), the driving task two types of outcomes are assumed to be realized: i) outcomes in the form of mobility/movement represented by a utility with no crashing ($U_{noCrashing}$); and ii) outcomes associated with safety represented by a utility of crashing ($U_{Crashing}$). It should be noted that in this type of formulation, additional types of outcomes may be considered including outcomes related to emission/power consumption. Starting with the basic formulation, a driver attempts to maintain a delicate balance between increasing his/her speed while ensuring that he/she does not crash. This act of balancing can be abstracted as the driver attempting to maximize his utility.

$$EU = P_{noCrashing}U_{noCrashing} + P_{Crashing}U_{Crashing} \tag{1}$$

The expected utilities here represent the working memory modules and the encoding process (Hastie and Dawes, 2010) as these utilities are not objective (as opposed to the utilities used in the standard utility maximization theory where rationality and complete information are assumed). The probabilities associated with each type of outcome are also subjective and can take the form on any risk-taking attitudes (i.e. under-estimating/over-estimating gains/losses). Based on Teiber at al. (2000) and Hamdar et al. (2008), the suggested "subjective" crashing probability at time $t + \tau$ (where τ is the anticipation time) is:

$$P_{Crashing}(t + \tau) = \Phi\left(\frac{\Delta v(t)\tau + 0.5a\tau^2 - s(t)}{\tau\sigma(v)}\right) \tag{2}$$

Where a is the current acceleration rate, *s(t)* is the space gap at time *t*, $\Delta v(t)$ is the relative velocity with respect to the lead vehicle at time *t* (i.e. $v(t) - v_{lead}(t)$). It is assumed that the uncertainty in the perception represented by $\sigma(v)$ increases with speed v and is represented by αv, where α is a constant parameter indicating the relative error in estimating speeds. Furthermore, we assume at this stage that the disutility of crash is a negative constant w_c:

$$U_{Crashing} = -w_c \tag{3}$$

Therefore, with $P_{noCrashing} = 1 - P_{Crashing}$ and assuming that both the non-crashing utility and the crashing probability depends on the actual acceleration a, we arrive at

$$EU = \left(1 - P_{Crashing}\right)U_{noCrashing} - w_c P_{Crashing} \tag{4}$$

It is assumed that a driver is a "total" subjective expected utility (*EU*) "maximiser", where utilities are associated with different action alternatives (i.e. in this case, an acceleration *a* is an alternative); the driver will attempt to maximize the *EU(a)* in Equation 4 at each time step. It can also be assumed that since the probability of a crash is very small, the term $P_{Crashing}U_{noCrashing}(a)$ will be very small and can be omitted in further analysis, since the probability of crashing is extremely low. For added explanation, $P_{Crashing}U_{noCrashing}$ is of the order $P_{Crashing}$ since $U_{noCrashing}$ is of the order one. However, w_c is of the order 10 000 (as will be shown in the feasibility analysis and the calibration phase): $P_{Crashing}w_c$ is about 10 000 times larger than $P_{Crashing}U_{noCrashing}$. Therefore, it is sensible to simultaneously neglect $P_{Crashing}U_{noCrashing}$ and not neglect $P_{Crashing}w_c$. Such neglection leads to,

$$\frac{dEU(a)}{da} = U'_{noCrashing}(a) - w_c P'_{Crashing}(a) = 0 \tag{5}$$

Using Equations (2) and (5) and the assumption $\sigma(v) = \alpha\, v$, we get the following general implicit equation for the acceleration a of a driver maximizing his or her total expected utility:

$$U'_{noCrashing}(a) - \Phi'\left(\frac{\Delta v(t)\tau + 0.5a\tau^2 - s(t)}{\alpha v}\right)\frac{\tau w_c}{\alpha v} = 0 \tag{6}$$

$$U'_{noCrashing}(a) = \frac{\tau w_c}{2\alpha v\sqrt{2\pi}}\mathrm{e}^{\frac{\left(\Delta v + 0.5a\tau - \frac{s - s_0}{\tau}\right)^2}{2\alpha^2 v^2}} \tag{7}$$

Under the assumption of steady state conditions, $\Delta v \to 0$ and $a \to 0$, therefore Equation 7 for a general utility model can be written as

$$s = s_0 - \alpha v\tau\sqrt{2\ln\left(\frac{\tau w_c}{2\alpha v\sqrt{2\pi}}\right) - 2\ln\left(U'_{noCrashing}(0)\right)} \tag{8}$$

The paper explores the implications of three different kinds of utility models for the acceleration-based models: *i)* Prospect Theory (PT), *ii)* Constant Relative Risk Aversion (CRRA), and *iii)* Exponential Constant Relative Risk Aversion (ECRA). The forms of the utility functions associated with the three aforementioned models have been widely used in microeconomics to evaluate risk attitudes. Furthermore, preferences among framed alternatives have been found to be significantly different in the loss domain than in the gain domain. Accordingly, the utility functions are formulated differently in the gain and loss domains. Due to this difference, the overall utility function has a kink (non-differentiable but continuous) at the reference point (zero). This paper proposes a smoothening method to ensure differentiability at "zero" for the various utility functions and their respective steady state conditions. The "zero" is assumed to be the current reference point (i.e. current time step) with respect to which the gains and losses (i.e. is speed) are being evaluated.

<u>Prospect Theory</u>

The utility function used in the prospect theory models is a normalized power function, where the exponent represents the risk attitudes. The utility functions are described in Tversky and Kahneman, (1986).

$$U(a) = \begin{cases} \left(\frac{a}{a_0}\right)^{\gamma_1} & a > 0 \\ -w\left(\frac{-a}{a_0}\right)^{\gamma_2} & a < 0 \end{cases} \tag{9}$$

w is the relative weight of losses in speed if compared to the same amount of gain in speed. In other words, if *w* = 3, the driver would perceive the loss in speed three times more than the gain in the same amount of speed (i.e. risk-aversion). γ_1 and γ_2 are relative non-linearity parameters controlling the derivatives of the value function at the acceleration distribution extremes (i.e. associated with the risk attitudes). The utility function is smoothed to ensure differentiability of *U(a)* at zero acceleration (i.e. no gains or losses in speed). a_o indicates the width of the smoothing method. Smoothing is needed both from a macroscopic fundamental diagram (FD) perspective and from a microscopic individual driver behavioural perspective. From a FD perspective, without a_o, the different initial utility forms suggested in this paper have a vertical gradient at $a = 0$. Accordingly, derivatives of the initial utility functions with respect to a cannot be calculated at $a = 0$ and thus, the FD is undefined for these initial utilities. From a driver behavioural perspective, the initial utilities also do not reflect real behaviour since vertical gradients mean infinite sensitivities which no human has; humans may have bi-stable/metastable responses but these responses are not a subject of study in this paper and they do not fall within the framework of driver behaviour. It should be noted that the magnitude of a_o (i.e. one can set $a_o = 1\ m/s^2$) does influence the results remarkably; changes of a_o can be compensated for by changes in w and/or γ_i(at least near the steady state). The utility function in Equation 9 is used in conjunction with Equation 8 to determine the steady-state relationship between spacing and speed as a function of the prospect theory parameters.

$$s(v) = s_0 + \sqrt{2}\alpha\tau v\sqrt{\left(1 - 0.5(\gamma_2 + \gamma_1)\right)\ln(a_0) + \ln\left(\frac{2}{1+w}\right) + \ln\left(\frac{\tau w_c}{2\alpha v\sqrt{2\pi}}\right)} \tag{10}$$

<u>*Constant Relative Risk Aversion (CRRA)*</u>

The CRRA utility function is defined by Equation 11. The exponent (γ_i) in the CRRA function represents the risk attitudes. The different risk attitudes over positive and negative accelerations reflect the different preferences over the loss and gain domain.

$$U(a) = \begin{cases} \frac{(a)^{1-\gamma_1}}{1-\gamma_1} & a > 0 \\ -\frac{(-a)^{1-\gamma_2}}{1-\gamma_2} & a < 0 \end{cases} \tag{11}$$

Again, using the smoothening technique proposed in the full paper in conjunction with Equation 8, the steady state condition under the assumption of the CRRA utility function is shown in equation 12.

$$s(v) = s_0 + \sqrt{2}\alpha\tau v\sqrt{\left(1 - 0.5(\gamma_2 + \gamma_1)\right) + \ln\left(\frac{\tau w_c}{2\alpha v\sqrt{2\pi}}\right)} \tag{12}$$

<u>*Exponential Constant Relative Risk Aversion (ECRA)*</u>

The ECRRA utility function is defined by Equation 13. The exponent (γ_i) in the ECRA function (Holt and Laury, 2000) represents the risk attitudes. Similar to the earlier case, the different risk attitudes over positive and negative accelerations reflect the different preferences over the loss and gain domain.

$$U(a) = \begin{cases} \frac{1-e^{-\kappa(a)^{1-\gamma_1}}}{\kappa} & a > 0 \\ -\frac{1-e^{-\kappa(-a)^{1-\gamma_2}}}{\kappa} & a < 0 \end{cases} \tag{13}$$

κ is the exponential power parameter that constitutes an added difference between the CRRA and the ECRA models. Again, using the smoothening technique in conjunction with Equation 8, the steady state condition under the assumption of the ECRA utility function is shown in equation 14.

$$s(v) = s_0 + \sqrt{2}\alpha\tau v\sqrt{\ln(\kappa) + \ln\left(\frac{\tau w_c}{2\alpha v\sqrt{2\pi}}\right)} \tag{14}$$

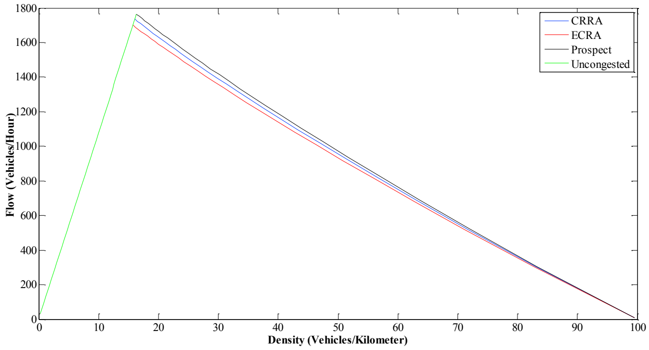

Fig. 2. The Fundamental Diagram for different utility functions.

It is interesting to note that the steady state equation for the ECRA utility was not affected by risk attitude parameters γ_1 and γ_2, while the other utility functions resulted in steady state equations impacted by the parameters representing the risk attitudes. In a non-car following mode the vehicles choose a free flow speed, otherwise the speed-density relationship is dictated by the steady state equations. The steady state equations for all three utility functions demonstrate a nearly triangular fundamental diagram, albeit with differences in capacity. This is shown in Figure 2. In addition to the macroscopic feasibility analysis to evaluate if the suggested models are consistent with well-known traffic phenomena, there is a need to perform a microscopic feasibility analysis, calibration and validation. Such microscopic aspect of this study aims at checking if the models are able to reproduce key traffic dynamics while connecting individual behaviour to collective traffic observations: such analytical connection is often missing when offering newer psychology or economics-based traffic flow models.

3.2. Micro-Feasibility Analysis

In the earlier formulation section, we focused on the general model structure (utility structure set up – Equations 1 through 8) and the steady state equations after smoothing the corresponding subjective utility functions (i.e. Equations 9 through 14). Investigating the model further at the individual driver behavioral level, Figure 3 offers the subjective utility functions associated with a given gain or loss in speed (i.e. acceleration or deceleration) with respect to a reference point (i.e. zero acceleration at current speed). These functions correspond to the parametric values presented in Table 1 (parameters explained in Equations 9 through 14). It should be noted that the suggested parametric values in this subsection reflect the average parameter value based on the calibration results (which will be discussed in detail in the next section). A preliminary sensitivity analysis to produce basic realistic following maneuvers is presented in Figure 4. Notice that the PT value function is not completely similar to the PT *tanh* functional form presented in Hamdar et al. (2015). This change in form is due to the decoupling of the positive and negative acceleration domains to create two separate functions (Equation 9) that are connected and smoothened at the “zero” reference point. However, given the weight parameter *w*, risk aversion is manifested in the larger absolute values of the dis-utilities in the negative acceleration domain if compared to the absolute values of the utilities in the positive acceleration domain. The exponents γ_i still produces a non-linearity where the relative added gains at the function’s extremes (for example, gaining 2 m/s in speed while traveling at 20 m/s) are valued less than the related added gains near the reference point (i.e. descending grade as we move to the extreme points in the positive acceleration domain). The opposite may be said regarding the PT negative acceleration domain.

Table 1. Subjective utility parametric values for micro-feasibility analysis.

Parameters\Models	PT ([min, max])	CRRA ([min, max])	ECRA ([min, max])
w	3.82 ([0.2, 9.4])	-	-
γ_1	0.81 ([0, 1.9])	0.31 ([0.0, 0.9])	0.35 ([0.2, 0.8])
γ_2	1.31 ([0.1, 1.9])	0.20 ([0.0, 0.8])	030 ([0.1, 0.9])
κ	-	-	0.60 ([0.1, 2.0])

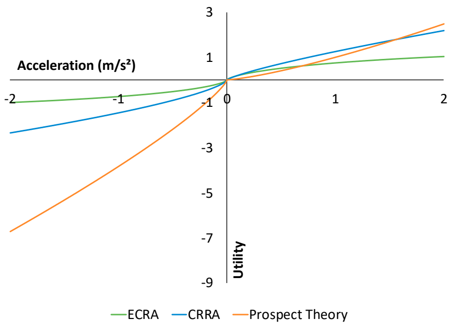

Fig. 3. Acceleration utility function for prospect theory (orange), CRRA (blue), and ECRA (green). All model parameters are selected based on calibration results.

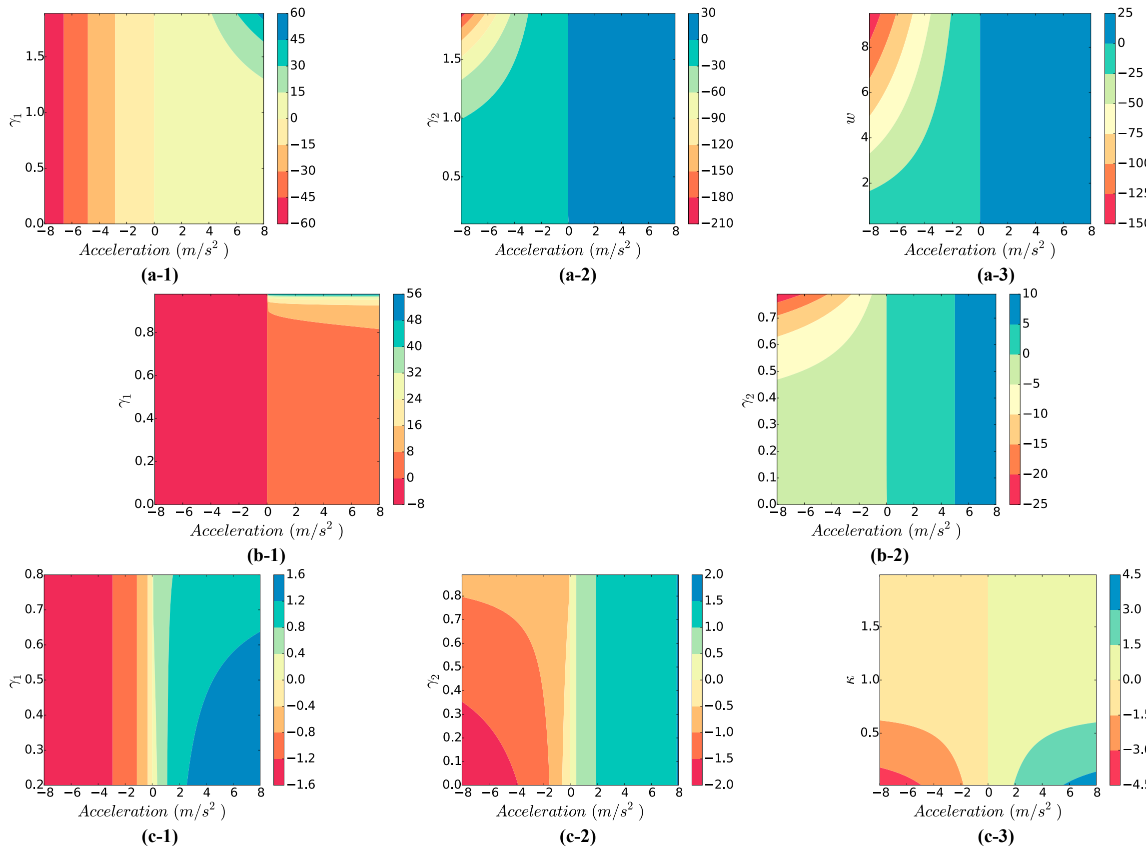

Fig. 4. Sensitivity of utility to various model parameters for prospect theory model (a-1 to a-3), CRRA (b-1 and b-2), and ECRA (c-1 to c-3).

Figure 5 translates the subjective utility functions (1st row of plots) into acceleration probability density functions (*pdf*s) (second row of plots) facing a certain leader behavior. The probability density functions corresponding to the PT (first column of plots), the CRRA (second column of plots) and the ECRA (third column of plots) when a driver is travelling at 10 mph and is separated from the leader by a 10 m spacing. Three types of dynamics are illustrated: *i)* approaching the leader with a relative velocity of +10 mph (green plots), *ii)* keeping a constant space headway with a relative velocity of 0 mph (orange line plots), and *iii)* increasing the space headway with the leader with a relative velocity of -10 mph (blue plots). As expected, approaching the leader will generate higher deceleration rates. However, the *pdf*s associated with the three functional forms presented in the formulation section are different in terms of mean/median (i.e. the peak of the distributions) and standard deviations (the range of the distributions). First, the

ECRA function produces non-bell shaped *pdf*s that may not be directly approximated by a normal distribution for added implementation ease. Moreover, the ECRA produces the highest deceleration rates in the three suggested driving scenarios mainly due to the exponential component amplifying the sensitivity to the gains/losses in speed. However, the exponential form of the utility function also produces the "widest" *pdf*s that are skewed to the right. On the other hand, both the PT and the CRRA value functions produced bell-shaped *pdf*s with the CRRA *pdf*s being characterized by slightly lesser accelerations (i.e. the CRRA acceleration means are lesser than the PT acceleration means) and wider distributions. In other words, more conservation behavior is seen in the CRRA formulation but with an added stochasticity illustrated in the wider choices available from the corresponding *pdfs*

To illustrate how the *pdf*s translate into acceleration choices, Figure 6 maps the *pdf*s for the PT model (1st Column), the CRRA model (2nd column) and the ECRA model (3rd column), into a three dimensional space with more diverse driving conditions. The 1st driving condition corresponds to a velocity of 10 mph and a spacing of 10 m while varying the relative velocity from 4 m/s (approaching the leader) to – 4 m/s (decelerating away from the leader). In all three models, as the driver approaches the leader, a higher deceleration rate is applied. The mean values are almost identical (~peak of the distributions) when comparing the PT model (Figure a-1) to the CRRA model (Figure a-2). However, more stochasticity is observed (thicker yellow line in Figure a-2) with the CRRA model. What is interesting is that the PT model shows relatively higher disturbance (i.e. more acceleration choices) in the positive acceleration domain than in the negative acceleration domain while the CRRA model shows higher disturbance in the -'ve acceleration domain than in the positive acceleration domain. The ECRA model results in the highest deceleration rates and the highest stochasticity consistently (Figure a-3). The second driving scenario (2nd column) corresponds to a relative velocity of 0 mph and a driver's speed of 10 mph. As we decrease the spacing from 17.5 m to 2.5 m between the two successive vehicles, the follower is expected to increase his or her deceleration rate (decrease his acceleration rate). Such result shows the validity of the modeling structure suggested earlier with the ECRA model showing the highest deceleration rates and stochasticity followed by the CRRA model followed by the PT model. Since there is no change from a positive to a negative acceleration in such driving scenario, no clear discontinuity exists in the CRRA and ECRA models' *pdf*s. Finally, the third driving scenario corresponds to a relative velocity of 0 mph and a spacing of 10 m. If the follower is travelling at a speed of 20 m/s (~40 mph), the 10 m spacing is not considered to be a safe spacing and an extreme deceleration rate is applied (lower bound of -4 m/s^2). If the follower's speed decreases, a higher acceleration rate may be applied. In terms of stochasticity reflected by the width of *pdf*s, we can see the same properties seen in the first driving scenario.

In summary, the three micro-economic based modeling formulations (PT, CRRA and ECRA) presented in Sub-section 3.1 show acceptable macroscopic homogeneous properties (i.e. triangular fundamental diagram and steady-state space-velocity relationship) and microscopic stochastic properties (i.e. accelerations rates properly associated with spacing, velocity and relative velocity with different acceleration *pdf*s' characteristics). The models allow capturing different risk-taking tendencies while incorporating unsafe behavioral patterns in incident/near-incident conditions. Such tendencies are further explored in the calibration exercise presented in the next section.

4. Data and Calibration

4.1. Data Description

One of the main contributions of the presented formulation is the ability to calibrate the weights associated with the risk-taking tendencies associated with each model through observed trajectory data. We utilize in this paper the Next Generation Simulation (NGSIM) data collected on Route 101 southbound (i.e. Hollywood Freeway) in Los-Angeles, California, USA, on the 15th of June of 2018. The route section observed is 640-meter in length and has 5 through lanes. An on-ramp (Ventura Boulevard) allows vehicles to access the freeway and an off-ramp (Cahuenga Boulevard) allows vehicle to exit the freeway. The on-ramp acceleration lane and the off-ramp deceleration ramp form a weaving right-hand auxiliary lane. Synchronized video cameras were mounted on a nearby 36-story building and a special software was used to extract the trajectory data for each vehicle passing through the observed freeway section. (Colyar and Halkias, 2007).

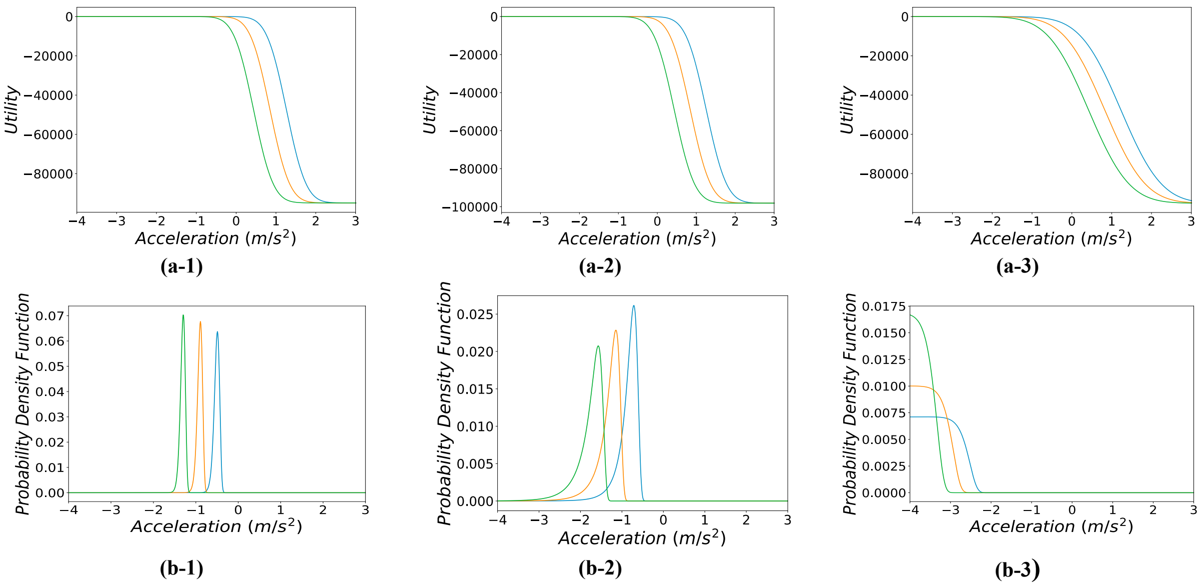

Fig. 5. Utility (a-1 through a-3) and probability density function (b-1 through b-3) for prospect theory model (a-1 and b-1), CRRA (a-2 and b-2), and ECRA (a-3 and b-3) for V = 10mph, s = 10m, and various values of ΔV (ΔV = -10mph is represented by blue line, ΔV = 0mph is represented by orange line, and ΔV = 10mph is represented by green line). All model parameters are selected based on calibration results.

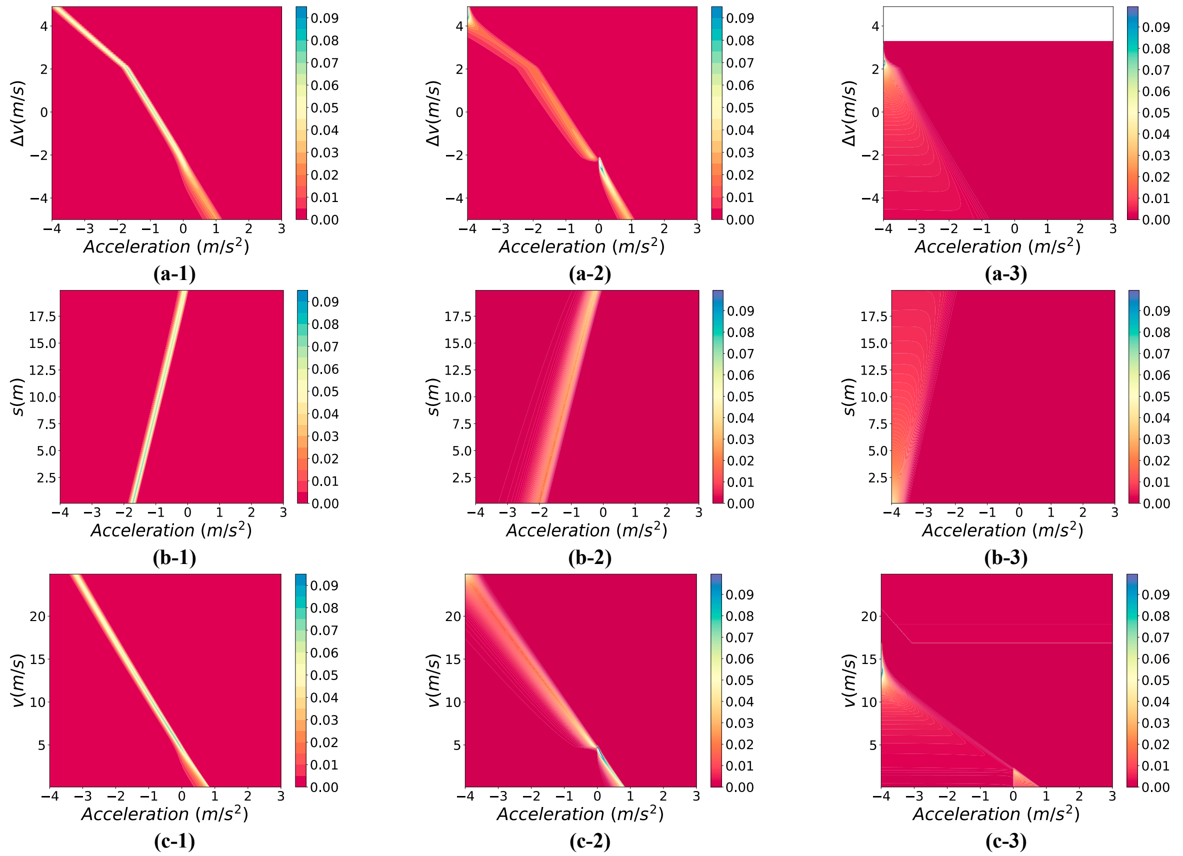

Fig. 6. Probability density function for (1) prospect theory model, (2) CRRA, and (3) ECRA. (a -1 through a-3) V = 10mph, s = 10m, (b-1 through b-3) ΔV = 0mph and V = 10mph, and (c-1 through c-3) ΔV = 0mph and s = 10m. All model parameters are selected based on calibration

The total data collection time on this section was 45 minutes with three 15-minute data collection periods: 7:50 am – 8:05 am; 8:05 am – 8:20 am and 8:20 am – 8:35 am. These periods coincide with the peak-hour AM commute time allowing the observation of the increase in flow, the traffic breakdown (i.e. transition from non-congested state to congested state), and the formation of different congestion dynamics. A total of 150 vehicle trajectories were extracted. The data sets include the longitudinal and lateral coordinates (representing the location of the center of the front-bumper of each vehicle), the vehicle ID, the vehicle type/dimension, an absolute and a relative time-stamp (with a 0.1 second resolution). Such information allowed the extraction of the speed, the acceleration, the relative velocity, the time/space headway and the spacing associated with each vehicle in each lane at every time-step. Such information were used in the model calibration presented in the next sub-section. The fundamental diagram and a snapshot space-time-velocity field associated with NGSIM Route 101 data are presented in Figure 7. As mentioned earlier, this figure showcases the existence of different congestion waves during the data collection period.

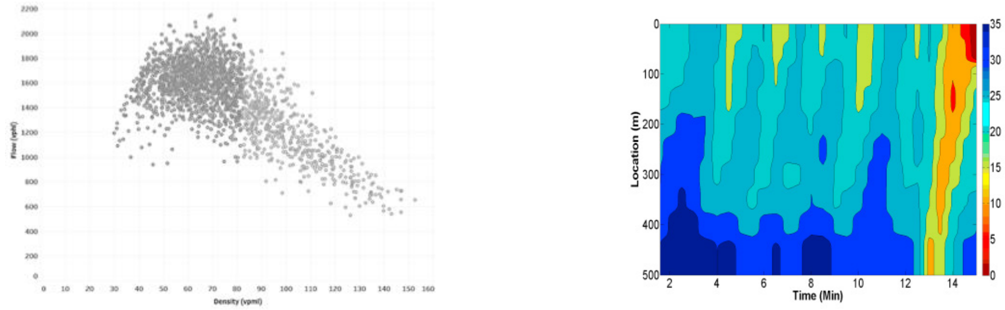

Fig. 7. Fundamental diagram (left) and space-time velocity field (right) associated with the trajectory observations during the data collection period.

4.2. Genetic Algorithm Calibration

Focusing on the non-homogenous traffic phenomena and the microscopic inter-vehicular interactions, finding an optimal parameter set for each of the car-following model formulation presented in Section 3 becomes a nonlinear optimization problem that needs to be solved numerically. Accordingly, a genetic algorithm calibration approach (Hamdar et al., 2009) is adopted while taking into account the inter-vehicle heterogeneity.

A direct comparison between the observed trajectories and the simulated trajectories using each of the aforementioned utility-based formulations (i.e. Section 3.1) is possible. In the simulation set-up, the calibration is performed by taking different leader-follower pairs and comparing their driving dynamics with the behavior obtained from the simulated car-following models. The simulated relative velocity and the distance gap are initialized to the empirically given relative velocity and gap.

$$\Delta v^{sim}(t=0) = \Delta v^{data}(t=0) \tag{15}$$

$$s^{sim}(t=0) = s^{data}(t=0) \tag{16}$$

The microscopic operational stage model is used to compute the acceleration and thus the trajectory of the following vehicle. The gap to the leading vehicle is computed as the difference between the simulated trajectory $x^{sim}(t)$ (front bumper position) and the recorded position of the rear-bumper of the leading vehicle $x_{leader}^{data}(t)$:

$$s^{sim}(t) = x_{leader}^{data}(t) - x^{sim}(t) \tag{17}$$

The above measure can be directly compared to the gap provided by the data $s^{data}(t)$.

Once the calibration performance measure (i.e. spacing) is identified, the kind of error to be minimized should be specified. The absolute error term is less sensitive to small deviations from the empirical data and the relative error term is more sensitive to small spacings than to large spacings. Accordingly, a mixed spacing error term will be utilized as the objective function to be minimized using the genetic algorithm calibration method. This mixed error term is defined as:

$$F_{mix}[s^{sim}] = \sqrt{\frac{1}{|s^{data}|} \langle \frac{(s^{sim} - s^{data})^2}{|s^{data}|} \rangle} \quad (18)$$

Where

$$\langle z \rangle = \frac{1}{\Delta T} \int_0^{\Delta T} z(t) dt \quad (19)$$

After defining the objective function, the genetic algorithm heuristic terms are presented as follows:

- A "chromosome" represents a parameter set of the car-following models and a population consists of N_{GA} such chromosomes.
- In each chromosome generation, the fitness of each chromosome is determined via the mixed term objective function defined earlier.
- All pairs of chromosomes are extensively generated from the current population and recombined to generate new chromosomes.
- The cross-over point where two chromosomes are combined is randomly selected.
- Except for the chromosome with the best fitness score, all the genes (model parameters) are mutated (varied randomly) following a given probability. The resulting chromosomes (new generation) are used in the next iteration.
- Initially, a fixed number of generations is evaluated. The evolution is then terminated when the best-of-generation score converges from one iteration to another for a given number of generations.

In this research, the initial set of parents (10 parents) is initiated where the parameters are given values in the proximity of those provided in the feasibility analysis phase of Section 3. At each iteration, these parents produce 90 children chromosomes where the best 10 candidates are kept to the next iteration. The calibration process continues until no improvement of more than 0.01 is observed for 20 consecutive iterations or when the error reaches the threshold of 20%. It should be noted that a mutation rate of 10% is applied in all iterations.

The total of 1000 vehicle trajectories were used for the calibration and validation of the results. To validate the calibration outcome, 80% of each trajectory is utilized for calibration and the remaining 20% is utilized for validation. Note that this approach is consistent with the findings of Kim and Mahmassani (2011) that model parameters in microscopic simulation models are expected to be correlated. Table 2 shows the calibration and validation results, including key model's variables and mixed spacing error (as calculated based on (18)). The error for validation is slightly higher than for calibration. In few cases, the validation shows that the calibration process has failed to capture the behavior. These cases are rare and correspond to the cases that the traffic flow regime is significantly different between the first 80% and the last 20% of the trajectory (e.g., free flow vs. stop and go). Overall, from an error perspective, PT model outperforms CRRA and ECRA. Table 3 shows the correlation matrixes for the three models. The correlation pattern is similar for the PT and CRRA models. γ_1 and γ_2 show a positive correlation in these models, indicating that more "aggressive" acceleration choices are associated with more "aggressive" deceleration choices. There is a weak correlation between γ_1 and w_c as well as γ_2 and w_c, indicating that crash weight is not clearly linked to the perception sensitivity to the losses or gains in speeds (i.e. positive or negative accelerations).

The correlation matrix is slightly different for the ECRA model though. γ_1 and γ_2 show a negative correlation, indicating that this model distinguishes between aggressive and timid drivers (i.e., drivers who favor acceleration vs. drivers who favor deceleration). There is also strong correlation between w_c and γ_1 as well as w_c and γ_2. γ_1 (representing the utility for positive acceleration values) has a positive correlation with w_c (representing the crash seriousness), indicating that with higher accelerations, drivers increasingly consider the possibility of being involved in a collision. On the other hand, γ_2 (representing the utility for negative acceleration values) has a negative correlation with w_c, indicating that drivers feel more comfortable (less crash risk) when decelerating.

Table 2. Calibration results (average values and standard deviation are presented for 1000 trajectories).

Parameters\Models	PT (SD; [min, max])	CRRA (SD; [min, max])	ECRA (SD; [min, max])
w	3.82 (2.65; [0.2, 9.4])	-	-
γ_1	0.81 (0.57; [0, 1.9])	0.31 (0.25; [0.0, 0.9])	0.35 (0.2; [0.2, 0.8])
γ_2	1.31 (0.48; [0.1, 1.9])	0.20 (0.12; [0.0, 0.8])	030 (0.21; [0.1, 0.9])
κ	-	-	0.60 (0.8; [0.1, 2.0])
w_c	97023.44 (21654.58; [50000, 143000])	98166.67 (16954.71; [50000, 140000])	96160.00 (24717.87; [50000, 140000])
Mixed Spacing Error (Calibration)	0.0730 (0.0261; [0.0249, 0.1451])	0.0758 (0.0290; [0.0225, 0.1391])	0.0836 (0.0371; [0.0229, 0.1465])
Mixed Spacing Error (Validation)	0.0840 (0.1134; [0.0049, 0.9150])	0.1259 (0.2217; [0.0099, 1.2858])	0.0986 (0.1314; [0.0123, 0.6547])

Table 3. Correlation matrix for (a) PT model, (b) CRRA model, and (c) ECRA model.

(a)

	γ_1	γ_2	w	w_c
γ_1	1.0	0.30	0.16	-0.06
γ_2	0.30	1.0	0.21	0.07
w	0.16	0.21	1.0	-0.01
w_c	-0.06	0.07	-0.01	1.0

(b)

	γ_1	γ_2	w_c
γ_1	1.0	0.22	-0.12
γ_2	0.22	1.0	-0.11
w_c	-0.12	-0.11	1.0

(c)

	γ_1	γ_2	κ	w_c
γ_1	1.0	-0.23	0.20	0.46
γ_2	-0.23	1.0	0.16	-0.13
κ	0.20	0.16	1.0	0.28
w_c	0.46	-0.13	0.28	1.0

5. Simulation Analysis

The first step in evaluating the performance of the proposed three models is focused on their ability to generate different traffic regimes. Accordingly, a one-lane ring road was simulated at different densities. Drivers' desired speed is set to 10 m/s. Note that with higher desired speeds, congestion can happen at lower densities and some intermediate flows regimes (between free-flow and fully congested) might not form. To create congestion, one vehicle enters the ring road between two consecutive vehicles at time t = 10s with the speed equal to half the desired speed. This vehicle may represent a merging vehicle entering the mainline from an on-ramp at a low speed.

Based on the calibration results, inter-driver heterogeneity is accounted for in this simulation exercise. The behavioral parameters associated with drivers' decision-making process (in terms of perception and judgement) in the microscopic simulation models are expected to be correlated. Kim and Mahmassani (2011) presented an effort to capture this correlation among the parameters of each driver. They showed that sampling from the empirical data while accounting for the correlation between the parameters of each sample (individual drivers) is the best method to capture heterogeneity in microscopic simulation models. In this study and based on their findings, the calibration results are used to generate the set of weakly or strongly correlated parameters. The correlated parameters from 150 vehicles are used to generate the parameters utilized in the simulation exercise. Based on the proposed method by Kim and Mahmassani (2011), the parameters of each generated vehicle in the simulation exercise are the same as the parameters of a particular vehicle recorded in the actual US 101 trajectory data.

Figure 8 shows the simulation results for densities equal to 30, 60, and 100 veh/km/lane. At a low density (30 veh/km/lane), the PT and CRRA models can absorb a given congestion wave (i.e. the disturbance does not propagate upstream and its magnitude diminishes by time). However, the ECRA model cannot absorb such waves as well as the other two models (i.e. it takes longer to contain the wave and then makes it dissipate). Moreover, with the ECRA model, additional shockwaves were created due to the amplification in the acceleration response as observed in Figures 5 and 6. As the density increases to 60 veh/km/lane, the difference in the car-following behavior among these models magnifies. The PT model results in one shockwave propagating upstream; however, no further shockwaves were created, and the created shockwave did not increase in bandwidth (i.e. thickness) impacting the entire traffic system. The ECRA model, on the other hand, resulted in a more widespread disturbance (lower speeds were observed at larger areas throughout the system). Finally, the ECRA model resulted in a stop-and-go traffic (i.e. multiple non-merged identifiable parallel waves) at this medium density value. This observation is consistent with the observations from the correlation matrix since the ECRA model produces more extreme acceleration values and high deceleration values amplifying the response to a given change in the relative velocity or the space headway. This is mainly due to the exponential component in the ECRA formulation and its manifestation as an exaggeration in the judgement process. At a higher density (100 veh/hr/lane – close to the jam density), the PT model results in stop-and-go traffic, while the other two models result in a fully congested system. Such observation confirms our prior findings from the micro-feasibility analysis: the ECRA produces more accentuated deceleration rates compared with the PT model while the CRRA model is associated with an added randomness and thus uncertainty in the acceleration choices leading to further disturbances (if compared to the PT model) and further congestion.

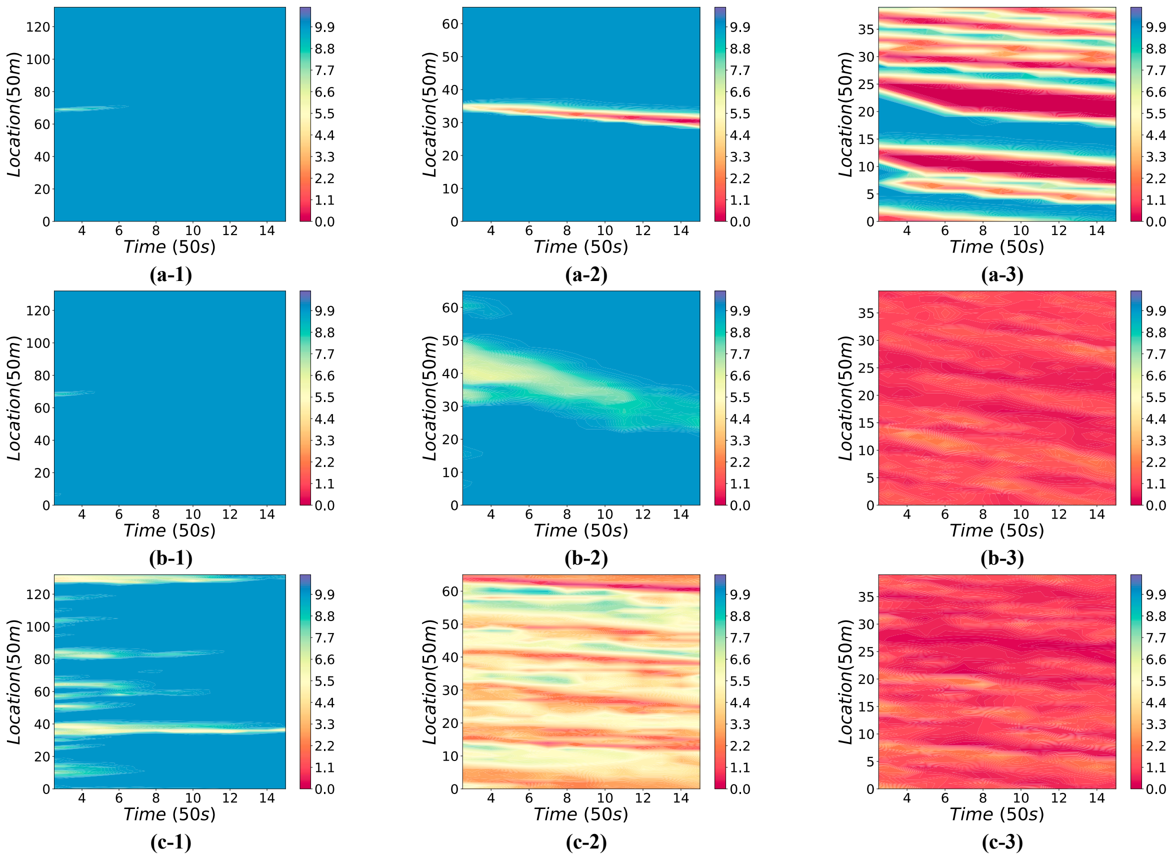

Fig. 8. Speed profile over time and space at density = 30 veh/km/lane (x-1, x = a, b, or c), density = 60 veh/km/lane (x-2, x = a, b, or c), and density = 100 veh/km/lane (x-3, x = a, b, or c) for (a) prospect theory model, (b) CRRA, and (c) ECRA. Desired speed is set 10mph.

For safety evaluation, Figure 9 shows the probability of adopting a given crash seriousness factor w_c (Equation 3) and a given estimated collision probability (Equation 2) by vehicles simulated with densities equal to 30, 60, and 100 veh/km/lane. The higher the $w_c.f_n$ product is (i.e. x-axis), an additional number of instances with unsafe behavior is observed leading to extreme accelerations and decelerations. Such higher $w_c.f_n$ products are seen in Figure 9-b. In other words, higher number of vehicles using the CRRA model adopts a high $w_c.f_n$ product leading to more extreme accelerations and decelerations and possibly errors. It is essential to note that the extreme accelerations and decelerations here are not the product of the non-collision component of the utility function (i.e. Equation 1); the exaggerated acceleration reactions are due to the collision component of the utility function counter-balancing the effect of the limited risk-averseness seen in the CRRA SUF. This combination between the limited risk-averseness and the collision sensitivity might explain the lack in transition between a free flow state and a fully congested state in Figure 8-b but may still be the reason behind collision formation even with a limited density level. When comparing Figure 9-a (PT) to Figure 9-c (ECRA), a higher number of vehicles considers a zero-estimated collision probability with the ECRA model leading to unsafe following of the lead vehicle followed by extreme deceleration. Such finding is in line with the findings presented in Figure 8 (higher disturbances at lower density levels).

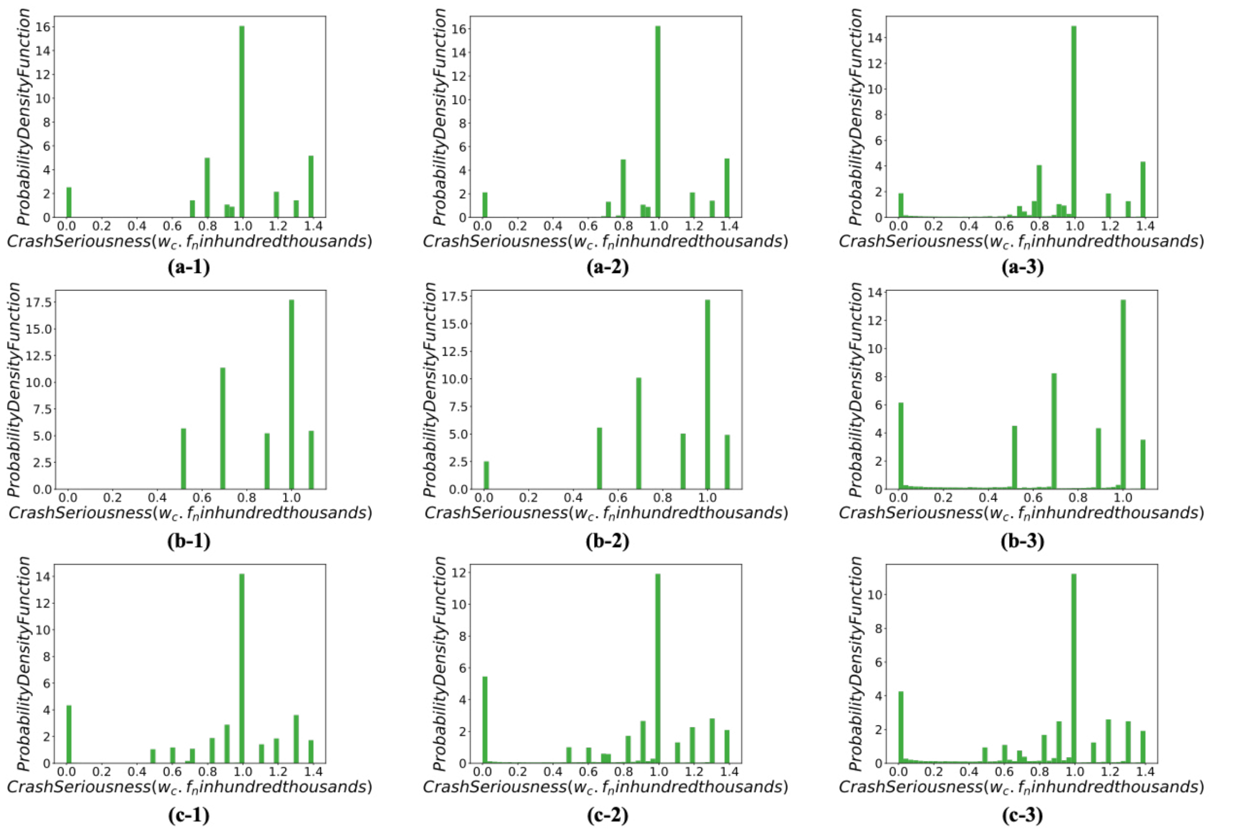

Fig. 9. Probability of adopting a collision probability function multiplied by a given CrashSeriousness Parameter w_c by vehicles simulated at density = 30 veh/km/lane (x-1, x = a, b, or c), density = 60 veh/km/lane (x-2, x = a, b, or c), and density = 100 veh/km/lane (x-3, x = a, b, or c) for (a) prospect theory model, (b) CRRA, and (c) ECRA.

6. Conclusions

The ultimate goal of this research effort is to provide a comprehensive numerically verifiable theory for utility-based car-following models. Apart from the methodological contributions (i.e. linking decision making theories to traffic flow theory) and the numerical contributions (i.e. formulating a numerically tractable calibration process and simulating real-world congestion dynamics) associated with these models, this study mainly addresses the following questions:

1- What type(s) of utility functions best describe observed microscopic and macroscopic traffic conditions?

2- How significant are the behavioural heterogeneities and what is their impact on traffic mobility and safety?

Answering Question 1: from a homogenous stable traffic conditions' standpoint, the different presented subjective utility functions (SUFs) produce realistic macroscopic triangular fundamental diagrams both through analytical derivation (i.e. integration method) and through simulation (inter-driver interaction replication). However, the dynamics produced when dealing with the non-homogenous traffic states/regions (i.e. delimited through congestion waves' formation, propagation and merger) are very different. Based on the micro-feasibility analysis and the simulation results, the Constant Relative Risk Aversion (CRRA) SUF along with the Prospect Theory (PT) SUF produced the most stable behavior without the quick formation of multiple waves at medium density levels (i.e. one single wave is observed). However, it is only with the PT model that well-delimited congestion bands are seen in the speed distribution maps offered in this paper. Such congestion bands with multiple shockwaves are seen at high density levels in the case of the PT model and at medium density levels in the case of the Expected Constant Relative Risk Aversion (ECRA) model. It should be noted that these multiple waves are observed when analyzing the Route 101 Next Generation Simulation (NGSIM) data used to calibrate the different proposed models. The Exponential Constant Relative Risk Aversion (CRRA) model resulted in more "chaotic" speed bands (even at low density levels) that may not be a characteristic of every-day recurrent commute congestion. Such finding may be explained given the modeling approach adopted in this paper (i.e. approach: a microeconomic modelling framework translated into a longitudinal driving behavior model that reflects the cognitive dimension of the driver decision-making process).

The ECRA model represents a driving behavior that is sensitive to the surrounding stimulus thus amplifying the response to either the leader getting further away (i.e. acceleration domain) or the leader being approached (i.e. the deceleration domain). It should be noted that the cause of such amplification is not the perception/sensory dimension (i.e. reflected by the relatively small weight associated with the gains and losses as plotted in Figure 3). The drivers adopting the ECRA "decision logic" are considered as risk-averse (thus the "risk aversion" nomenclature when referring to ECRA utilities) and have constant rate of increase in the weights associated with the alternatives being evaluated (i.e. thus the "constant" nomenclature when referring to the ECRA utilities). The cause of the amplification is attributed to the decision making/judgement process (as defined by the Information Processes/Process Theories presented both in Figure 1 and in Section 2). The exaggeration in the response is mainly due to the exponential term (i.e. Equation 13) as this constitutes the main different between the ECRA model and the CRRA model. Based on the calibration results and the error distributions across vehicles, we can state that the ECRA model produced smaller errors than the CRRA model possibly indicating the ECRA's utility better describes the microscopic traffic conditions observed on Route 101 (based on the utilized NGSIM trajectory data set). This is also attributed to the fact the ECRA function reproduces different congestion waves as seen in the Route 101 NGSIM data while the CRRA model does not show a transient phase moving from a single wave to a homogeneous congestion region (i.e. Figure 9-b). However, the ECRA's judgement module may be better suited for traffic modeling during extreme conditions (near collision or evacuation scenarios) with the drivers still showing a rational behavior (i.e. all the models presented in this model are considered to be within the realm of rational models given their micro-economic utility-based construct). In other words, even though the calibration results and the macro and the micro analysis of the formulation suggests the suitability of both the ECRA and the PT models, the simulation results show the superiority of the PT model for every day car-following modeling. Such superiority is further validated through the lower PT calibration errors.

Comparing the CRRA model with the PT model, the main difference is attributed to the intra-driver heterogeneity reflected by the added randomness (i.e. wider acceleration probability distribution function) seen in the CRRA model (i.e. Figures 5 and 6). However, the risk-averseness is accentuated in the PT SUF as seen in Figure 2 (i.e. a higher weight attributed to the losses in speed when comparing the CRRA and the PT models). Moreover, the PT model shows an anisotropy when comparing the weights between the "loss" domain and the "gain domain". Such accentuated risk-averseness and anisotropy overcome the added randomness and the wider acceleration distribution functions seen in the CRRA model. Risk averseness and anisotropy may be the main cause of the added stochasticity seen in the PT model and thus the added PT disturbances observed in the corresponding simulated speed maps. In conclusion, we claim that the PT SUF is more representative of driver behavior when congestion is manifested and that drivers are risk averse in nature during every-day commute conditions. However, when the traffic conditions become more challenging, risk-averseness and sensitivity increases in possibly ECRA judgement during extremely challenging traffic conditions.

Answering Question 2: as explained earlier, intra-driver heterogeneity may be manifested through the perception/judgement stochastic process rather than the changes in the models' parameters depending on the traffic condition at hand. In other words, the models suggested in this paper are inherently stochastic (the models' final output is an acceleration probability density function – *pdf* – rather than a single acceleration value) and are able to capture the intra-driver heterogeneity observed during different instances of the driving episodes. Given the limited cumulative error level seen in the calibration exercise (for all three models), we claim that intra-driver heterogeneity should be seen as a natural outcome of the decision-making process rather than being forced by changing the models' parameters at different times of a given driver's trip. This hypothesis results in a more tractable calibration approach and an additional ease when implementing and analyzing a given car-following model. The main type of heterogeneity that is manifested in this paper is however the inter-driver heterogeneity. Such heterogeneity is clearly seen in Section 4 and is a major factor transforming the homogeneous fundamental diagram (i.e. Figure 2) into a traffic system with scattered flow density data points and different congestion regimes (i.e. Figure 9). In other words, it is the intra-driver risk-averse stochastic decision-making process and the inter-driver heterogeneity that results in the different congested regimes and the corresponding shockwave formation, propagation, merger and dissipation (thus producing different congested states). The inter-driver heterogeneity is then an added contributor to the capacity drop and the decrease in safety leading to additional near-incident scenarios. It should be noted that we can create all congestion states by just changing the demand/supply boundary values when setting up any simulation exercise. The capacity to recreate such states is a necessary condition to claim that a car-following model is acceptable and reproduce rear-world congestion dynamics. However, the behavioral reasoning associated with the transition between such states especially when not controlling for the boundary conditions are what remain unexplained numerically and through simulation. This paper claims that the stochastic risk-averse decision-making processes are the behavioral reasons leading to the transitions between different traffic states and are the main drivers for human errors and incident formation.

In summary, this paper does not simply utilize a given utility function (for example, a *tanh* form of a prospect theory – PT – subjective utility function – Hamdar et al., 2015) to produce additional simulation results. An alternative formulation construct is offered with a direct comparison between well-established SUFs made possible. For implementation purposes, the resulting formulated SUFs were smoothened and made differentiable rendering the asymptotic approximation possible for implementation and calibration purposes. The SUFs were then integrated into a micro-economic stochastic framework (resulting in acceleration *pdf*s) while allowing for perception and judgement errors leading to possible rear-end collisions. Accordingly, this paper develops a construct to offer multiple utility-based forms that may capture acceleration behavior while calibrating and simulating the corresponding models. The initial PT model of Hamdar et al. (2015) is modified and framed in a more general context of behavioural economics with different variants. As an outcome, the CRRA SUF was based on a re-formulation of the PT SUF; moreover, a new ECRA SUF formulation is presented and analyzed microscopically and macroscopically. The resulting methodological formulation is further supported by an elaborate empirical and simulation study: a more elaborate calibration and validation showcases the ability of recreating different congestion dynamics while capturing inter-driver heterogeneity and intra-driver stochasticity. With such modelling approach, driver behavioural elements were introduced into the acceleration modelling research allowing the understanding of certain traffic phenomena as an outcome of individual risk-prone drivers' decision-making processes. Simpler physics based, or stimulus-response acceleration models need phenomenological driving characteristics as a direct input. However, the association to the human behavioural dimensions remains somewhat unclear. The offered models directly connect such dimensions, particularly risk attitude, with the driving style, particularly with the desired time gap. This can be directly used *(i)* to investigate how different driver personalities influence the efficiency and the stability of traffic flow, and *(ii)* to develop adaptive-cruise-control subsystems of automated vehicles which feel comfortable for a given personality.

Despite the findings made in this study, we acknowledge that further work is still possible along this line of research (i.e. incorporating cognitive dimensions into the driving decision-making process). For example, further calibration and simulation runs may be made while attributing different decision-making logic (i.e. SUFs) to different drivers. Moreover, the authors may conduct extended simulation effort while reproducing additional safety metrics. Such rates may be then compared to rear-world collision rates calculated through mining through both traffic detector and collision data repositories. This may lead to additional insights answering *Question 2* presented in this Conclusions Section. Finally, the flexible formulation framework presented in this paper may be further expanded to take into account *i)* different expected utility forms, *ii)* additional traffic performance measures, and *iii)* alternative gain/loss coding methods.

Acknowledgements

This material is based upon work supported by the National Science Foundation under Award No. 1351647. Any opinions, findings, and conclusions or recommendations expressed in this material are those of the author(s) and do not necessarily reflect the views of the National Science Foundation.

References

Ahmed, K. I., 1999. Modeling Driver's Acceleration and Lane Changing Behaviors. Ph.D. Dissertation, Department of Civil and Environmental Engineering, Massachusetts Institute of Technology, Cambridge, Massachusetts, USA.

Atkins, 2016. Research on the Impacts of Connected and Autonomous Vehicles (CAVs) on Traffic Flow. Summary Report, Version 1.1, UK Department of Transport, May 2016.

Arbis, D., Dixit, V. V., Rashidi, T. H., 2016. Impact of risk attitudes and perception on game theoretic driving interactions and safety. Accident Analysis and Prevention, Vol. 94, pp. 135-142.

Barthélemy, J-P., Coppin, G., Lenca, P., 2006. COGNITIVE APPROACH TO DECISION MAKING AND PRACTICAL TOOLS. IFAC Proceedings Volumes, Vol. 39, Issue 4, pp. 123-128.

Bhat, C. R., Steed, J. L., 2002. A continuous-time model of departure time choice for urban shopping trips. Transportation Research Part B: Methodological, Vol. 36, Issue 3, pp. 207-224.

Camerer, C. F., 2011. Behavioral Game Theory: Experiments in Strategic Interaction. Princeton University Press, Princeton, New Jersey, USA.

Chankong, V., Haimes, Y. Y., 2008. Multiobjective Decision Making: Theory and Methodology. Dover Publications, Inc., Mineola, New York, USA.

Childress, S., Nichols, B., Charlton, B., Coe, F., 2015. Using an Activity-Based Model To Explore Possible Impacts Of Automated Vehicles. Transportation Research Record: Journal of Transportation Research Board, Vol. 2493, DOI: 10.3141/2493-11.

Chorus, C. G., 2012. Regret theory-based route choices and traffic equilibria. Transportmetrica A., Vol. 8, Issue 12, pp. 291-305.

Colyar, J., Halkias, J., 2007. US Highway 101 Dataset. Federal Highway Administration (FHWA) Report No FHWA-HRT-07-030 (https://www.fhwa.dot.gov/publications/research/operations/07030/).

Dixit, V. V., 2013. Psychophysical Derivation of the Two-Fluid Model. Transportation Research Part C, Vol. 35, pp. 115 – 126.

Easley, D., Kleinberg, J., 2010. Modeling network traffic using game theory. In Networks, Crowds, and Markets: Reasoning about a Highly Connected World, Cambridge University Press, pp. 230-247.

Federal Highway Administration (FWHA), 2004. NGSIM Task E.1-1: Core Algorithms Assessment. Next Generation Simulation (NGSIM) Project, Final Report, Cambridge Systematic, Inc., Massachusetts.

Frydman, C., Camerer, C. F., 2016. The Psychology and Neuroscience of Financial Decision Making. Trends in Cognitive Sciences, September 2016, Vol. 20, No. 9, pp. 661-675.

Gerberg, G. B., 2002. Regret Theory – Explanation, Evaluation and Implications for the Law. University of Michigan Journal of Law Reform, Vol. 36, Issue 1, pp. 183-207.

Guala, F., Mittone, L., 2005. Experiments in economics: Testing theories vs. the robustness of phenomena. Journal of Economic Methodology, 12, pp. 495-515.

Hamdar, S. H., Treiber, M., Mahmassani, H. S., Kesting A., 2008. Modeling Driver Behavior as a Sequential Risk Taking Task. Transportation Research Record, No. 2088, pp. 208-217.

Hamdar, S. H., M. Treiber, Mahmassani, H. S., 2009. Calibration of a Stochastic Car Following Model Using Trajectory Data. National Research Council (U.S.), Transportation Research Board Meeting (88th: 2009: Washington, D.C.). Preprint CD-ROM.

Hamdar, S. H., Mahmassani, H. S., Treiber, M., 2015. From behavioral psychology to acceleration modeling: Calibration, validation, and exploration of drivers' cognitive and safety parameters in a risk-taking environment. Transportation Research Part B: Methodological, Vol. 78, pp. 32-53.

Hastie, R., Dawes, R. M., 2010. Rational Choice in an Uncertain World: The Psychology of Judgment and Decision Making. 2nd Edition, SAGE Publications, ISBN-13: 978-1412959032.

Holt, C. A., Laury, S. K., 2002. Risk aversion and incentive effects. American Economic Review, 92(5), 1644–1655.

Hoogendoorn, R., Van Arerm, B., Hoogendoorn, S., 2014. Automated Driving, Traffic Flow Efficiency, and Human Factors – Literature Review. Transportation Research Record, No. 2422, pp. 113-120.

Hranac, R., Gettman, D., Toledo, T., Kovvali, V., Alexiadis, V., 2004. NGSIM Task E.1-1: Core algorithms assessment, final report. Federal Highway Administration (FHWA) Report No FHWA-HOP-06-009.

Hwang, C-L., Masud, A. S. Md., 1979. Multiple Objective Decision Making – Methods and Applications: A State-of-the Art Survey. Lecture Notes in Economics and Mathematical Systems, Ed. Breckman and Kunzi, Springer-Verlag, Berlin Heidelberg, Germany.

Iyers, S., Reyes, J., Killingback, T., 2014. An application of evolutionary game theory to social dilemmas: The traveler's dilemma and the minimum effort coordination game. PLOS One, DOI: 10.1371/journal.pone.0093988.

Jaber, X., O'mahoney, M., 2009. Mixed stochastic user equilibrium behavior under traveler information provision services with heterogeneous multiclass, multicriteria decision making. Journal of Intelligent Transportation Systems, 13(4), pp. 188-198.

Jiang, X., Ji, Y., Du, M., Deng, W., 2014. A Study of Driver's Route Choice Behavior Based on Evolutionary Game Theory. Computational Intelligence and Neuroscience, DOI: 10.1155/2014/124716.

Kebabjian, R., 2018. Statistics: Causes of Fatal Accidents by Decade. Plane Crash Info (http://planecrashinfo.com), May 2018 (accessed on May 15, 2018: http://planecrashinfo.com/cause.htm).

Kim, J., Mahmassani, H. S., 2011. Correlated parameters in driving behavior models: Car-following example and implications for traffic microsimulation. Transportation Research Record, No. 2249, pp. 62-77.

Krisher, T., 2018. Safety investigators boot Tesla from probe into fatal crash of SUV on autopilot. USA Today (report from Associated Press), April 2018 (accessed on April 15, 2018: https://www.usatoday.com/story/money/cars/2018/04/12/safety-investigators-boot-tesla-probe-into-fatal-crash-suv-autopilot/512110002/).

Levin, S. T., 2018. Video released of Uber self-driving crash that killed woman in Arizona. The Guardian, March 2018 (accessed on March 30, 2018: https://www.theguardian.com/technology/2018/mar/22/video-released-of-uber-self-driving-crash-that-killed-woman-in-arizona).

Mahmassani, H. S., Koppelman, F., Frei, C., Frei, A., Haas, R., 2013. Synthesis of traveler choice research: Improving modeling accuracy for better transportation decision-making. Federal Highway Administration (FHWA) Report No FHWA-HRT-13-22.

Mahmassani, H. S., Liu, Y.-H., 1999. Dynamics of commuting decision behavior under advanced traveler information systems. Transportation Research Part C: Emerging Technologies, Vol. 7, Issue 2-3, pp. 91-107.

Mintz, A., Sofrim, A., 2017. Decision Making Theories in Foreign Policy Analysis. Oxford Research Encyclopedia of Politics, DOI: 10.1093/acrefore/9780190228637.013.405.

Moraes Ramos, G., Daamen, W., Hoogendoorn, S., 2011. Expected Utility Theory, Prospect Theory, and Regret Theory Compared for Prediction of Route Choice Behavior. Transportation Research Record, No. 2230, pp. 19-28.

Moraes Ramos, G., Daamen, W., Hoogendoorn, S., 2013. Modelling travellers' heterogeneous route choice behavior as prospect maximizers. Journal of Choice Modeling, 6, pp. 17-33.

Moraes Ramos, G., Daamen, W., Hoogendoorn, S., 2014. A state-of-the-art Review: developments in utility theory, prospect theory and regret theory to investigate travellers' behavior in situations involving travel time uncertainty. Transport Reviews, 34(1), pp. 46-67.

National Highway Traffic Safety Administration (NHTSA), 2016. 2015 Motor Vehicle Crashes: Overview. National Highway Traffic Safety Administration, Publication DOT HS 812 318. Washington, D.C.

Ohnsman, A., 2018. LiDAR Maker Velodyne 'Baffled' By Self-Driving Uber's Failure To Avoid Pedestrian. Forbes, March 2018 (accessed on March 27, 2018: https://www.forbes.com/sites/alanohnsman/2018/03/23/lidar-maker-velodyne-baffled-by-self-driving-ubers-failure-to-avoid-pedestrian/#6e1aa7c25cc2).

Ramos, G. de O., Bazzan, A. L. C., da Silva, B. C. 2018. Analyzing the impact of travel information for minimising the regret of route choice. Transportation Research Part C: Emerging Technologies, Vol. 88, pp. 257-271.

Rasouli, S. and Timmermans, H. J. P., 2014. Activity-based models of travel demand: Promises, progress and prospects. International Journal of Urban Sciences, 18(1), pp. 31-60.

Roth, A. E., 2002. The economist as engineer: Game theory, experimentation, and computation as tools for design economics. Econometrica, 70(4), pp. 1341-1378.

Saifuzzaman, M., Zheng, Z., 2014. Incorporating human-factors in car-following models: a review of recent developments and research needs. Transportation Research Part C: Emerging Technologies, Vol. 48, pp. 379–403.

Saifuzzaman, M., Zheng, Z., Haque, M. M., Washington, S., 2017. Understanding the mechanism of traffic hysteresis and traffic oscillations through the change in task difficulty level. Transportation Research Part B: Methodological, Vol. 105, pp. 523–538.

Stanovich, K. E., 2012. On the distinction between rationality and intelligence: Implications for understanding individual differences in reasoning. In Holyoak, K. and Morrison, R. (Eds.), The Oxford handbook of thinking and reasoning. New York: Oxford University Press, pp. 343-365.

Stanovich, K. E., West, R. F., Toplak, M. E., 2014. Rationality, intelligence, and the defining features of Type 1 and Type 2 processing. In Sherman, J. W., Gawronski, B. and Trope, Y. (Eds), Dual-process theories of the social mind. New York: Guilford, pp. 80-91.

Strack, P., Viefers, P., 2014. Regret and economic decision-making. VOX CEPR Policy Portal, 16 October 2014 (https://voxeu.org/article/regret-and-economic-decision-making - accessed November 12, 2018).

Talebpour, A., Mahmassani, H. S., Hamdar, S. H., 2015. Modeling lane-changing behavior in a connected environment: A game theory approach. Transportation Research Part C: Emerging Technologies, Vol. 59, pp. 216-232.

Teproff, C., Neal, D. J., 2018. Their lives ended 16 days before high school graduation - Speed might've been a factor. Miami Herald, May 2018 (accessed on May 10, 2018: http://www.miamiherald.com/news/local/community/broward/article210756349.html#storylink=cpy).

Treiber, M., Hennecke, A., Helbing, D., 2000. Congested traffic states in empirical observations and microscopic simulations. Physical Review E, 62, 1805.

Treiber M, Kesting, A., Helbing, D., 2006. Delays, Inaccuracies and Anticipation in Microscopic Traffic Models. Physica A 360, pp. 71-88.

Tversky A., Kahneman, D., 1986. Rational Choice and the Framing of Decisions. Journal of Business, Vol. 59, Issue 4, Part 2, pp. 251-278.

Van Lint, J. W. C., Calvert, S. C., 2018. A generic multi-level framework for microscopic traffic simulation – Theory and an example case in modelling driver distraction. Transportation Research Part B: Methodological, Vol. 117, pp. 63-86.

Walting, D. P., Cantarella, G. E., 2015. Model representation & decision-making in an ever-changing word: The role of stochastic process models of transportation systems. Network and Spatial Economics, 15(3), pp. 843-882.

Wiedemann, R., Reiter, U., 1992. Microscopic Traffic Simulation, the Simulation System Mission. Project ICARUS, Final Report. Brussels, CEC.

Xue, H., Zhou, J., Xu, W., 2011. A decision-making rule for modeling travelers' route choice behavior based on cumulative prospect theory. Transportation Research Part C: Emerging Technologies, Vol. 19, Issue 2, pp. 218-228.